Pharm Res (2015) 32:3986–3998
DOI 10.1007/s11095-015-1759-2

RESEARCH PAPER

Drug Release and Targeting: the Versatility of Polymethacrylate Nanoparticles for Peroral Administration Revealed by Using an Optimized *In Vitro*-Toolbox

Susanne Beyer[1] • Aline Moosmann[2] • Astrid S. Kahnt[3] • Thomas Ulshöfer[4] • Michael J. Parnham[4] • Nerea Ferreirós[5] • Sylvia Wagner[2] • Matthias G. Wacker[1]

Received: 30 April 2015 / Accepted: 15 July 2015 / Published online: 28 July 2015

ABSTRACT

Purpose The contribution of permeability and drug release to drug targeting were investigated in the course of development of a nanosized formulation of the anti-inflammatory compound TMP-001, for the local treatment in the gastrointestinal tract.

Methods TMP-001 was encapsulated by nanoprecipitation into Eudragit® RS 100. The permeability of these carriers was investigated in an Ussing chamber model and the release rate was determined under biorelevant conditions. Formulation toxicity and particle-cell-interaction were investigated by flow cytometry, fluorescence and electron microscopy. Furthermore, spray drying was performed.

Results Effective internalization of Eudragit®-nanoparticles into cancer cells was demonstrated. A burst release of the nanoparticles implied poor interaction of TMP-001 with Eudragit®. A sustained release (70.5% release after 30 min compared to 98.0% for the API) was accomplished after spray drying yielded an increased particle size. Recovery rate of TMP-001 after spray drying was 94.2±5.9%.

Conclusion The release of API from polymeric nanoparticles contributes profoundly to the *in vivo*-performance of drug delivery devices in the gastrointestinal tract. The impact of drug-polymer interaction and particle size was analyzed. Sustained release of TMP-001 could only be achieved by increasing particle size. Therefore, biorelevant release testing has been demonstrated to be a valid tool for nanoformulation design.

KEY WORDS biorelevant release · Eudragit® RS 100 · nanoparticles · peroral drug delivery · Ussing chamber

ABBREVIATIONS

API	Active pharmaceutical ingredient
CLSM	Confocal laser scanning microscopy
COX-2	Cyclooxygenase-2
DAPI	4′,6-Diamidin-2-phenylindol
DMEM	Dulbecco's Modified Eagle Medium
FCS	Fetal calf serum
GI	Gastrointestinal
mTHPC	Meso-tetrakis(3-hydroxyphenyl)chlorin
MWCO	Molecular weight cut-off
PBS	Phosphate buffered saline
PCS	Photon correlation spectroscopy
PDI	Polydispersity index
PTFE	Polytetrafluoroethylene
rpm	Rotations per minute
SD	Standard deviation
SEM	Scanning electron microscopy
TEM	Transmission electron microscopy
WST	Water soluble tetrazolium

INTRODUCTION

Polymeric nanocarrier devices are well-known for their beneficial characteristics enabling drug targeting, the improvement

✉ Matthias G. Wacker
wacker@em.uni-frankfurt.de

[1] Institute of Pharmaceutical Technology, Goethe University, Max-von-Laue-Str. 9, 60438 Frankfurt (Main), Germany

[2] Department of Bioprocess Technologies & Nanotechnology, Fraunhofer Institute for Biomedical Engineering, Ensheimer Straße 48, 66386 St. Ingbert, Germany

[3] Institute of Pharmaceutical Chemistry, Goethe University Frankfurt, Max-von-Laue-Str. 9, 60438 Frankfurt (Main), Germany

[4] Fraunhofer Institute of Molecular Biology and Applied Ecology, Project Group for Translational Medicine and Pharmacology, Theodor-Stern-Kai 7, 60596 Frankfurt (Main), Germany

[5] Institute of Clinical Pharmacology, Goethe University Hospital, Theodor-Stern-Kai 7, 60596 Frankfurt am Main, Germany

of bioavailability, and a reduction of side effects of an active pharmaceutical ingredient (API) (1–3). Regarding the multitude of application routes encompassing the parenteral, dermal, and peroral route of administration, it is obvious that characteristics of the nanocarriers have to be tailored carefully according to the pathophysiology of the addressed body compartment.

Concerning the peroral route of administration, diverse mechanisms of action must be taken into account. On the one hand side, chronically inflamed bowel disease and tumors in the gastrointestinal (GI) tract require penetration into inflamed tissues and an efficient internalization into specific cell types, such as immune-related or cancer cells (4,5). In this context, mucoadhesiveness and a sustained release of the API from the carrier can help to increase residence time at the specific site of action (6,7). On the other hand, API that exhibit a poor aqueous solubility are good candidates for nanosized formulations due to the increased dissolution rate and the altered GI transit time compared to dosage forms larger in size (3,8).

Previous studies have provided evidence that a certain amount of the nanocarriers can be taken up in its particulate form in the intestine by either paracellular transport in case of particles smaller than 50 nm or the endocytotic pathway (9,10). However, overcoming the intact mucus barrier that is characterized by a thickness of up to 830 μm is hard to achieve due to the dense network of the mucin glycoproteins (11). Nevertheless, diffusion through the pores of the mucin fibre matrix is possible for particles smaller than 100 nm and a neutral surface charge (12,13). Moreover, the size of perorally administrated formulations is essential if targeting of microfold cells is addressed as discussed for vaccinations (14). Schmidt *et al.* detected a pronounced transport of poly(lactide-co-glycolide) nanoparticles across inflamed colonic mucosal specimens that was not observed for microparticles of the same material (15). Hence particle diameter impacts biodistribution crucially.

Considering a local treatment in the GI tract, there is still a lack of profound knowledge in the way particle properties affect the applicability of nanocarriers for this purpose. Besides the accomplished impact of particle diameter, size distribution, and surface charge that all contribute to the extent particles are internalized into cells; the selected excipients for the generation of polymeric nanocarriers cannot be neglected (15–17). Regulating the interaction with specific cell lines and release properties, the interaction of API and polymer appears to be one key parameter explaining those complex mechanisms (18). Since it is evident that a fast dissolution of the API from the polymeric shell will limit the benefits nanoencapsulation is associated with, *in vitro*-tools for the physicochemical characterization have to be tailored to the addressed pathophysiological patterns.

The present research investigates the *in vitro*-performance of Eudragit® RS 100-based nanoparticles relying on a logical set of analytical methods, e.g., photon correlation spectroscopy (PCS), cell culture-based evaluation of the efficacy after processing of the API, microscopy and flow cytometry for studying the interaction of polymeric nanocarriers with GI specific cell lines.

The Ussing chamber model, known as a valuable tool for the prediction of GI permeability and absorption, was used for the evaluation of API and particle properties and their interaction with cell barriers producing mucus (19). Furthermore, biorelevant release testing was applied in order to investigate the interactions between drug, nanocarrier and the physiological environment, and their impact on the drug delivery paradigm. In this context, Eudragit® RS 100-nanoparticles were prepared by a scalable nanoprecipitation technique (20). Unloaded nanoparticles and a formulation containing the weak acid TMP-001 (pKa = 4.22, logP = 10.417) were investigated (20,21). TMP-001 is a model compound tested for its therapeutic relevance for several inflammatory diseases. The S-enantiomer of TMP-001 is a potent COX-2 inhibitor with anti-inflammatory properties and a high permeability. Aspiring an effective treatment, internalization into immune related cells is considered as beneficial (4,22). Due to an increased paracellular permeability induced by the disruption of tight junctions e.g., in inflammatory bowel disease, mucoadhesive dosage forms exhibiting a controlled release of the API are considered as promising formulations (6,23). In this context, the achievement of a prolonged release of the API at the specific site of action was intended.

For other compounds such as the photosensitizer temoporfin, a slow release from the polymeric shell and low systemic availability combined with an effective uptake of the loaded nanoparticles into cancer cells are considered to be beneficial (20,24). Recently, budesonide was effectively delivered to the inflamed colonic mucosa after incorporation into Eudragit® S-coated chitosan-Ca-alginate-microparticles. An erosion-controlled sustained release and a pronounced swellability were described as predominant factors for the release of the API at the specific site of action for this formulation (25). Another formulation based upon Eudragit® RL 100 containing clodronate also demonstrated sustained release properties (4). The presence of mucin in the release medium triggered the release of this API from the polymeric shell.

Depending on the interaction of API and polymer, varying release profiles can be assumed for polymeric nanoparticles of the same excipient. A strong interaction of drug and polymer combined with a favorable ratio of absorbed to encapsulated drug, can assure a prolonged release in spite of the short diffusion pathways in nanoscaled formulations (26). However, due to the large surface area, prolonged release characteristics are hard to achieve. In this regard, altered diffusion pathways can be considered one option in order to modify those patterns. Nevertheless, the potential for drug targeting relying on an increased penetration depth of nanocarriers into the gut wall is highly dependent on particle size and distribution

(15,27,28). Consequently, the augmentation of diffusion pathways in favor of release properties will attenuate the potential particle-cell interactions. It is also essential to contemplate release in the GI tract in the context of permeability, since both characteristics contribute to the *in vivo*-performance even when local treatment is required (4,29,30).

The presented research encompasses a systemic approach towards evaluation and adaption of particle characteristics of polymethacrylate-based formulations with regard to the encapsulated compound.

MATERIALS AND METHODS

Materials

TMP-001 (lot 5532052) was purchased from Aesica Pharmaceuticals Ltd. (Northumberland, UK). Pluronic F-68 (lot 8N009192) and 4′,6-Diamidin-2-phenylindol (DAPI; lot 3B002134) were purchased from AppliChem GmbH (Darmstadt, Germany). Eudragit® RS 100 (lot E100108020) was kindly provided by Evonik Röhm GmbH (Darmstadt, Germany). Polytetrafluoroethylene (PTFE)-syringe filters with a molecular weight cut-off (MWCO) of 0.1 μM were purchased from Whatman (Maidstone, UK). Dulbecco's Modified Eagle Medium (DMEM), heat-inactivated fetal calf serum (FCS), penicillin-streptomycin solution and DMEM/F12, penicillin-streptomycin, L-Glutamin were purchased from PAA Laboratories GmbH (Egelsbach, Germany) and Invitrogen (Karlsruhe, Germany), respectively. FCS was obtained from Sigma Aldrich (Steinheim, Germany). T-84 cell line was obtained from CLS (Eppelheim, Germany). Cell proliferation reagent water soluble tetrazolium (WST-1) was purchased from Roche Diagnostics (Mannheim, Germany). Concanavalin A, Alexa Fluor® 488 conjugate (lot 1154193) was purchased from Invitrogen (Eugene, USA). Lumogen® F Red 305 and Lumogen® F Orange 240 were kindly provided by BASF AG (Ludwigshafen, Germany). Carbogen LAB was obtained from Linde Gas (Mainz, Germany). FaSSIF V2 was kindly provided by biorelevant.com (Croydon, UK). Osmium tetroxide 4% solution (lot 080583), Araldit® CY 212 (lot 080623), Araldit® hardener Hy 964 (lot 071335) were purchased from Serva Electrophoresis GmbH (Heidelberg, Germany). Vectashield® fluorescence mounting medium was purchased at Vector Laboratories (Burlingame, USA).

Methods

Preparation of TMP-001-loaded Eudragit® RS 100-Nanoparticles

An amount of 15 mg TMP-001 and 150 mg Eudragit® RS 100 were dissolved in 1 mL ethanol 96% [*v*/*v*] at a stirring rate of 550 rpm. An aqueous Pluronic® F-68 solution with a concentration of 0.01% [*w*/*v*] was added dropwise with a peristaltic pump to these solutions and induced the formation of nanoparticles by precipitation. The flow rate was adjusted to 12 mL/min. The suspensions were stirred overnight. For the evaluation of cellular uptake, particles were additionally stained with Lumogen® F Red 305 and Lumogen® F Orange 240, respectively. In this context, an amount of 500 μg of the dye was added to the organic solution before precipitation.

Determination of Particle Properties by Photon Correlation Spectroscopy

A Zetasizer Nano ZS (Malvern Instruments GmbH, Malvern, UK) with a backscatter detector at an angle of 173° served for the determination of particle size and polydispersity index (PDI). Additionally, the zeta potential was measured by microelectrophoresis in a Malvern dip cell. Therefore, the suspensions were diluted 50-fold with purified water and transferred into a polystyrol cuvette.

Visualization of Particle Shape and Size by Electron Microscopy

For transmission electron microscopy (TEM), a volume of 20 μL of the nanocarrier suspension was transferred onto a coated copper grid. Staining of the polymer was achieved by incubation with phosphotungstic acid solution (2% [*w*/*v*]). The device used was a transmission electron microscope CM 12 (Philips, Amsterdam, The Netherlands) equipped with a Gatan module 782 (ES 500 W).

For the visualization of particles by scanning electron microscopy (SEM), an aliquot of 20 μL of the particle suspension was pipetted onto a sample holder and dried for 24 h. Afterwards, an Agar Sputter Coater (Agar Scientific, Essex, UK) was used for sputtering the particles with gold. Pictures were recorded with an Hitachi S4500 microscope system (Hitachi, Tokyo, Japan) at an accelerating voltage of 15 kV.

Determination of Drug Loading Efficiency and Particle Concentration

For the quantification of drug load, a volume of 200 μL of the particle suspensions was centrifuged through centrifugal filters (Amicon® Ultra, Millipore, Tullagreen, Ireland) containing a membrane of regenerated cellulose with a MWCO of 100 kDa. With the help of this procedure an effective separation of particles from the supernatant and therefore encapsulated from free API, was accomplished (20). Filter adsorption was tested under comparable conditions. The centrifugate was diluted and analyzed for the amount of API by an HPLC method adjusted from the one described by Akhlaq *et al.* in 2011 (31). The HPLC-system consisted of an LC-Organizer (Chromaster, VWR Hitachi, VWR International), a 5310

column oven, a 5430 diode array detector, a 5260 auto sampler and an 5160 intelligent pump. A reversed phase column (Gemini NX-C 18) was used as stationary phase. The mobile phase consisted of an aqueous solution of Na_2HPO_4 (30 mmol/L) and acetonitrile mixed at a ratio of 1:1. Flow rate was set to 1 mL/min, a wavelength of 247 nm was selected for detection. Linearity was assured in the range of 0.05 to 50 µg/mL. The amount of nanoparticles in the suspensions was determined gravimetrically. Therefore, the weight of the aluminum dishes was determined and 50 µL of the nanoparticle suspensions were pipetted onto each dish. The samples were dried to constant weight at a temperature of 80°C and incubated in an exsiccator overnight. The weight was determined after this procedure and the additional weight correlated to the amount of polymeric nanoparticles in the suspension.

Determination of Toxicity by WST-1 Assay

The cell viability assay was performed on HCA-7 and Caco-2 cells. Therefore, 15,000 cells per well were seeded into 96-well plates. Cells were allowed to attach for 24 h at 37°C and 5% CO_2. The medium was removed and 100 µL of the nanoparticle suspensions diluted in white DMEM were pipetted into each well. The applied concentrations ranged from 0.05 to 3 mg/mL loaded Eudragit® RS 100 nanoparticles (4,32,33). After 3 h of incubation the medium was removed and replaced with fresh white DMEM. A volume of 10 µL of WST-1 reagent was added and a further incubation of 1 h was performed. The microplate reader Infinite 200 PRO (Tecan Group Ltd., Männedorf, Switzerland) was used for evaluation of cell viability. A wavelength of 450 nm was selected for measurement, the reference wavelength was set to 620 nm.

Determination of the Efficacy of TMP-001-Loaded Nanoparticles by Evaluation of COX-2 Inhibition in HCA-7 Cells

The efficacy of TMP-001-loaded nanoparticles was tested in HCA-7 cells that express cyclooxygenase-2 (COX-2) constitutively. For those experiments the enantiopure S-form of TMP-001 was used, because its activity on COX-2 is 100fold more distinct compared to the racemate. Nanoparticles containing the S-form of TMP-001 were prepared as described herein. HCA-7 cells were grown in 6-well plates (500,000 cells per well) and various concentration of pure S-TMP-001 and the nanocarrier formulation were applied. Concentrations of 5 and 10 µmol/L of the API or the corresponding formulation diluted in DMEM were tested. After 2 h of incubation, the medium was transferred into caps and centrifuged at 2000 rpm for 5 min to separate cells from the supernatant. Samples were kept on ice and the supernatant was analyzed by LC-MS/MS for the amount of PGE_2 as an indicator for COX-2 inhibition.

Evaluation of Particle-Cell Interaction by Flow Cytometry of TMP-001-Loaded Nanoparticles and Caco-2 Cells

A number of 10^6 cells of Caco-2 cells (passage no. 9–12) were grown in 24-well plates. After 24 h, cells were washed and Lumogen® F Red-stained nanoparticles containing TMP-001 were diluted in DMEM and 1 mL applied to the wells utilizing concentrations of 100, 250, and 500 µg/mL. After 2 h cells were harvested with trypsin-EDTA solution. The reaction was stopped with cell culture medium after 5 min. The cell suspensions were transferred into caps and centrifuged for 5 min at 1200 rpm. The supernatant was decanted and cells were resuspended in 100 µl PBS containing 1% [*v*/*v*] FCS. The cells were fixed and centrifugated for 5 min at 1200 rpm. The pellet was subsequently resuspended in PBS. The cell suspensions were filtered through the cell strainer caps of BD falcon tubes and measured with the device BD FACSAria™III (Becton Dickinson Biosciences, Franklin Lakes, USA). 10,000 events were measured and the shift in fluorescence intensity (median) that corresponds to the Texas Red channel was used for the evaluation of uptake and interaction of the nanoparticles with cells.

Determination of Cellular Uptake of Eudragit® RS 100-Nanoparticles with the Help of Fluorescence Microscopy

Caco-2 cells that were at passage no. 7 were grown on cultures slides (BD Falcon®, Thermo Fisher Scientific Inc., Waltham, USA) to a density of 10,000 cells/cm^2. A concentration of 50 µg per mL medium of the nanoparticles (unloaded or TMP-001-loaded, both stained with Lumogen® F Red 305) were applied to each chamber containing 10,000 cells. After incubation for 2 h, the cell membrane was stained with an Alexa Fluor® 488 conjugate of succinylated Concanavalin A, DAPI was used for staining of the nucleus. After washing of the cell layers and sealing with Vectashield® fluorescence mounting medium, visualization was achieved with the microscope AxioImager Z1 microscope and Axiovision 4.6 software (Zeiss, Göttingen, Germany).

Qualitative Evaluation of Cellular Uptake of Unloaded Eudragit® RS 100-Nanoparticles by Transmission Electron Microscopy

Caco-2 cells were grown in DMEM containing 10% [*v*/*v*] FCS and penicillin-streptomycin at 37°C and 5% CO_2. Cells that were at passage no. 15 to 17 were seeded on a coverglass (50,000 cells/cm^2) and allowed to adhere for 24 h. Cell layers were incubated with unloaded Eudragit® RS 100-nanoparticles at a concentration of 50 µg/mL, diluted in DMEM medium containing 10% [*v*/*v*] FCS, for 2 h.

Subsequently, pre-fixation by incubation with a solution of glutardialdehyde (2.5% [*v/v*]) in phosphate buffered saline solution (PBS; pH 7.4) was conducted. After washing with PBS, post-fixation was achieved with a solution of osmium tetroxide (1% [*v/v*]) in PBS for 2 h. Dehydration of the cell layer with ascending concentrations of ethanol and embedment into Araldit® resin was performed according to the method described by Zensi *et al.* (34). After complete infiltration of the resin into the cell layer, and hardening of the resin was assured, the cover glass was removed and sections were obtained with an Ultra S microtome (Leica Microsystems GmbH, Wetzlar, Germany). A diatome knife ultra 45° (Schmied Labortechnik, Bielefeld, Germany) was used for cutting into ultrafine sections. A double staining procedure with uranyl acetate and lead citrate was performed in order to contrast the polymeric nanocarriers, and a transmission electron microscope CM 12 (Philips, Amsterdam, Netherlands) was used for visualization.

Spray Drying of the Nanocarrier Suspension and Characterization of the Obtained Powder

The Mini-Spray dryer B-290 (Büchi Labortechnik AG, Essen, Germany) equipped with a three-fluid nozzle of an inner diameter of 0.7 mm (item no. 046555) was used for achieving a solid powder. The nanoparticle suspensions were mixed with a mannitol solution to a final concentration of 5% [*w/v*] for the sugar alcohol. The nanocarrier suspensions were delivered to the nozzle at a pumping speed of 6.25 mL/min. The aspirator was operated at 100%. Inlet temperature was regulated to 75°C; the outlet temperature was monitored to be 35 ± 1°C throughout the process. This process was performed for the TMP-001-loaded particles. The obtained powder was dissolved in ethanol 96% [*v/v*] and analyzed for the amount of TMP-001 by HPLC-analysis. The amount of Eudragit® RS 100 was determined by size exclusion chromatography as described by Porsch *et al.* (35). In this context an HPLC-system composed of an LC-Organizer (Chromaster, VWR Hitachi, VWR International), a 5310 column oven, a 5450 refractive index detector, a 5260 auto sampler and an 5160 intelligent pump was used. As stationary phase a Biosep SEC-s3000 column (Phenomenex Inc., Aschaffenburg, Germany) was used with a mobile phase consisting of LiCl (100 mM) dissolved in ethanol 96% [*v/v*].

Permeability Studies Conducted with the Ussing Chamber Model

Transport studies with the Ussing chamber model were performed with the intestinal cell line T-84 derived from lung metastases of human colon carcinoma. The accomplished cell layers produce mucin. The cells were cultured on Transwell® inserts (3 μm pore size, polycarbonate-membrane) (Corning, Wiesbaden, Germany) for 2 weeks before they were utilized for experiments. 300,000 cells were seeded per Transwell® and cultured at 37°C and 5% CO_2 at a humidity of 85%. The membranes with the grown cells were placed into inserts in the Ussing chamber (Physiologic Instruments, San Diego, USA). The effective membrane area comprised 0.33 cm^2. The chamber halves were filled with Tyrode's buffer (pH 6.8) and oxygenated with carbogen. The transepithelial resistance was monitored throughout the experiment. Nanoparticle suspension, spray dried powder, or free drug were added to the mucosal compartment and incubated for 3.5 h. The concentration of the API TMP-001 in the mucosal compartment was adjusted to 20 μg/mL. Samples were collected from both compartments, serous and mucosal, and stored at −20°C until HPLC-analysis. The permeability rate after 3.5 h of all tested formulations was determined by regarding the permeated amount of TMP-001 over time in the context of the effective membrane area. Therefore, the amount of API that crossed the T-84 cell layer in the relevant time interval was divided by the concentration of API that remained in the donor compartment and the effective membrane area. Hence the result was expressed by the unit of [10^{-4} cm/s] that is also used for permeability coefficients.

For the blank, Lumogen® F Orange-loaded Eudragit® RS 100, Transwell® membranes were cryoembedded in Tissue Tek® (Sakura Finetek Europe BV, AJ Alphen aan den Rijn, Netherlands) for the visualization with confocal laser scanning microscopy (CLSM). Therefore concentrations of 10 and 20 μg/mL, respectively were applied into the donor compartment. Consequently, cryosections of the cell membranes with a thickness of 10 μm were prepared. The sections were transferred onto microscope slides and mounted with mounting medium containing DAPI. Sections were analyzed with a Leica CLSM (Wetzlar, Germany).

Release Experiments Performed in the Biorelevant Medium FaSSIF V2

In order to determine the release properties of the established formulations containing TMP-001, the sample-and-separate technique was used. Therefore, an USP-2 apparatus (ERWEKA DT 6 R, ERWEKA GmbH, Heusenstamm, Germany) equipped with mini vessels and mini paddles (ERWEKA DT 600, ERWEKA GmbH, Heusenstamm, Germany) was employed. A volume of 300 mL FaSSIF V2 medium was used; the stirring speed was set to 75 rpm. Temperature was kept constant in the range of 37 ± 0.5°C. The biorelevant dissolution medium FaSSIF V2 was prepared by dissolving 1.79 g FaSSIF V2 powder in maleic acid buffer pH 6.5. After complete release was achieved, the volume was adjusted to 1 L with the mentioned buffer system. An amount of 10 mg of TMP-001 or the corresponding amounts of the nanosized or spray dried formulations were used for release experiments. Dissolution tests were run for 4 h. After

defined time intervals, samples of 1.5 mL volume were removed and replaced with fresh medium. Samples were subsequently pushed through filters with an MWCO of 0.1 μm (Anotop 25, Whatman International Ltd., Maidstone, UK). The first 500 μL were discarded. The amount of the TMP-001 was determined by HPLC. Filter absorption was tested beforehand. The cumulative amount released was expressed as percentage of the theoretical concentration gained by 100% drug release.

Statistical Analysis

All data are expressed as mean ± standard deviation (S.D.). For the determination of significance, Kruskal-Wallis One Way Analysis of Variance on Ranks was performed. An all pairwise multiple comparison procedure was performed with the help of Holm-Sidak method. Differences were considered to be significant if $p < 0.05$.

RESULTS

Characterization of Nanoparticles by Photon Correlation Spectroscopy

The characterization of nanocarriers by PCS revealed a mean diameter of 171.1 ± 3.3 nm and a monodisperse size distribution as indicated by a PDI of 0.189 ± 0.014 for the unloaded Eudragit® RS 100 nanocarriers. The zeta potential as an indicator of surface charge was determined to be +51.3 ± 3.4 mV. In case of TMP-001-loaded particles the zeta potential was increased to values of +64.2 ± 4.8 mV while no influence on size and size distribution was detected. Incorporation of the dye Lumogen® F Red 305 did not affect the described properties neither when it was incorporated solitarily, nor after encapsulation besides TMP-001.

For the API an encapsulation efficiency of 98.1 ± 1.9% was determined by HPLC after separation of nanoparticles from the supernatant. An absolute drug load of 98.1 ± 1.9 μg TMP-001 per mg nanoparticles was achieved resulting in a drug loading capacity of 9.8% [*w*/*w*].

The excipient composition assured optimal characteristics of the nanocarrier formulation with regards to particle size, size distribution, zeta potential, and encapsulation efficiency as described previously (20). Further characterization was undertaken in order to make sure that TMP-001 had no effect on relevant product characteristics of the selected formulation design.

Visualization of Nanoparticles by Electon Microscopy

Observations by TEM and SEM ascertained spherical shape of TMP-001-loaded nanoparticles and confirmed the diameter measured by PCS (see Fig. 1a and b). Their visual appearance was identical to particle systems synthesized from the same polymeric material as published previously (20). There were no residues of crystalline API observed.

Determination of Toxicity by WST-1 Assay

Since the interactions with cellular surfaces can have an influence on the uptake, degradation, and drug release from the nanocarrier devices, these parameters have been investigated. By assessing cytotoxicity of the TMP-001-loaded drug delivery system, an effect of reduced cell viability on further experiments was excluded. Consistent with some earlier findings concentrations in a range between 0.05 to 3 mg/mL of the TMP-001-loaded nanoparticles were tested on Caco-2 and HCA-7 cells (4,32,33).

No decrease in cell viability was recognized in neither of these cell lines after 4 h (see Fig. 2a). Even at high concentrations of the API there was no sign of apoptosis detected (see Fig. 2a). Moreover, the drug-loaded nanocarriers were comparable in their toxicity to their unloaded counterparts.

Determination of the Efficacy of TMP-001-Loaded Nanoparticles by Evaluation of COX-2 Inhibition in HCA-7 Cells

The TMP-001-loaded nanocarriers were analyzed with regards to the therapeutic efficacy of the API after encapsulation into the drug delivery system. The S-enantiomer of the compound TMP-001 as an effective COX-2 inhibitor was able to reduce the amount of PGE_2 in the supernatant significantly (see Fig. 2b). After processing this API by encapsulation into Eudragit® RS 100, the extent of COX-2 inhibition remained consistent. For both, the unprocessed API and the nanoparticles, the lowest concentration of 5 μM already diminished the amount of PGE_2 to values below 30% compared to the control (unloaded Eudragit® RS 100-nanoparticles).

Evaluation of Particle-Cell Interaction by Flow Cytometry of TMP-001-Loaded Nanoparticles and Caco-2 Cells

In order to determine the interaction of the nanocarrier systems with Caco-2 cells quantitatively, flow cytometry analysis was undertaken (see Fig. 2c). Referring to the median-shift of the Texas Red signal, cell adhesion or alternatively cellular internalization of nanoparticles depended on the concentration of applied nanoparticles and the incubation time. At low concentrations (100 $\mu g/10^6$cells) there was still a certain amount of cells that did not carry the Texas Red signal and were consequently not in interaction with the nanocarriers. Correlating with increasing particle concentrations, the fluorescence signal was intensified.

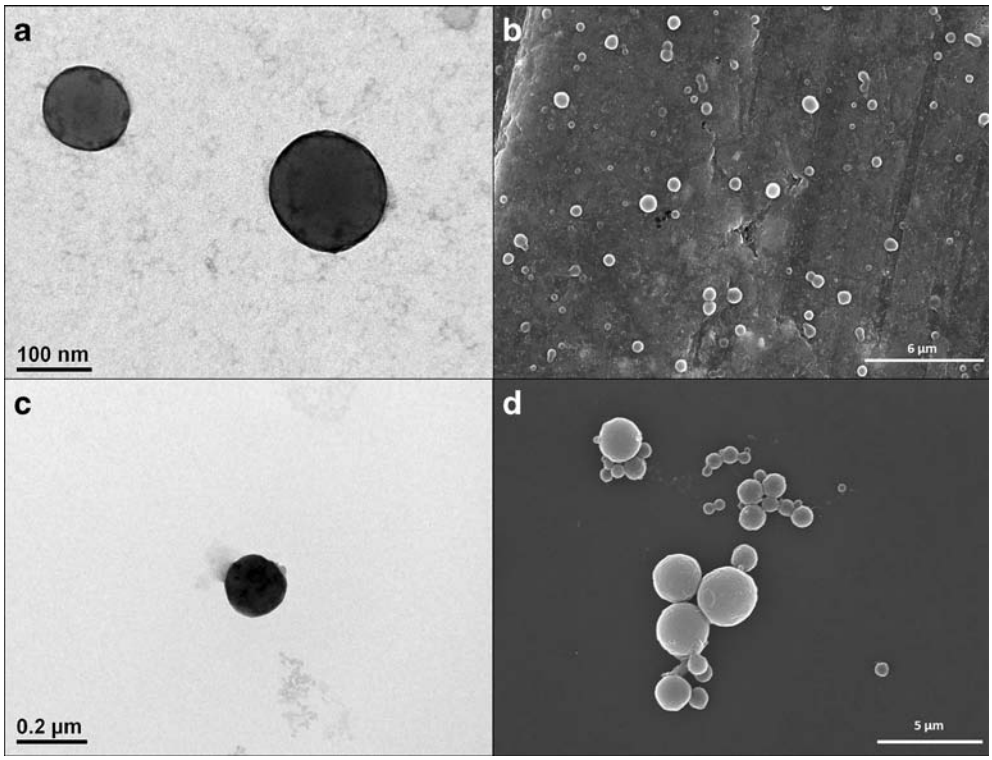

Fig. 1 TMP-001-loaded Eudragit® RS 100 nanoparticles visualized before (**a**, **b**) and after spray drying (**c**, **d**) by TEM (**a**, **c**) and SEM (**b**, **d**). Agglomerates were formed during the spray drying procedure (**d**).

Determination of Cellular Uptake of Eudragit® RS 100-Nanoparticles with the Help of Fluorescence Microscopy

Since flow cytometry analysis revealed strong association between nanocarrier system and the respective cell lines, fluorescence microscopy was performed in order to confirm internalization of the nanoparticles into the cytoplasm. The red color of the stained nanoparticles could be recognized in the cytoplasm of the Caco-2 cell layers (see Fig. 3a and b).

This effect appeared to be comparable for the unloaded nanoparticles and the TMP-001-loaded particles (see Fig. 3a and b).

Qualitative Evaluation of Cellular Uptake of Unloaded Eudragit® RS 100-Nanoparticles by Transmission Electron Microscopy

Aiming to provide a general evidence for the internalization of the prepared nanoparticles into the cytoplasm, the interaction of unloaded nanocarriers with Caco-2 cells was visualized by

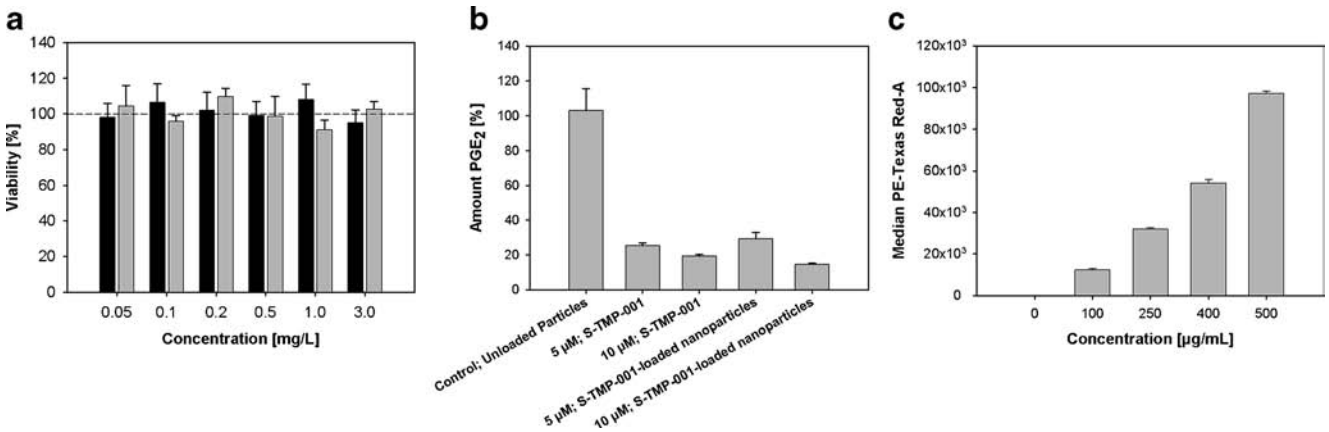

Fig. 2 (**a**) Viability of HCA-7 (*grey*) or Caco-2 (*black*) cells determined by WST-1 assay after incubation with TMP-001-loaded nanoparticles for 4 h. All experiments were performed in triplicate. S.D. is used for descriptive *error bars*. (**b**) Flow cytometry of 10^6 Caco-2 cells that were incubated with varying concentrations of Lumogen® F Red 305-labeled nanoparticles containing TMP-001. All experiments were performed in triplicate. S.D. is used for descriptive *error bars*. (**c**) The extent of COX-2 inhibition by the S-enantiomer of TMP-001 or nanoparticles containing S-TMP-001. As an indicator the amount of PGE_2 in the supernatant of HCA-7 cells was quantified by LC-MS/MS. All experiments were performed in septuplicate. S.D. is used for descriptive error bars.

TEM. The obtained pictures after slicing of Caco-2 cells, which were embedded into Araldit® resin, assured that nanoparticles entered the cytoplasm. As seen in Fig. 4a–d, the endocytosis of Eudragit®-particles can be assumed to be one important factor in the delivery of Eudragit® RS-nanoparticles.

Spray Drying of the Nanocarrier Suspension and Characterization of the Obtained Powder

In order to investigate the impact of an increase in particle size on the *in vitro*-performance, microparticles were prepared by spray drying of the nanosuspensions. Controlling the process parameters of the spray drying procedure, lead to a recovery of 94.2±5.9% of the API and of 90.9±6.2% of Eudragit® RS 100 in the obtained powder (related to the ratio of API to excipients in the suspension used for spray drying). Visualization by TEM revealed that larger agglomerates were formed during the process that was accompanied by a polydisperse size distribution (see Fig. 1d). However, still particles with a size lower than 200 µm were preserved (see Fig. 1c).

Permeability Studies Conducted with the Ussing Chamber Model

Permeability, as a meaningful factor for the performance of nanocarriers in the GI tract, was investigated by means of the Ussing chamber model.

The Ussing chamber model assured a permeation of 10.05 ±1.5% for the unprocessed API TMP-001 from the mucosal into the serous compartment. Over a time period of 3.5 h a permeation rate of $1.236 \pm 0.1402 * 10^{-4}$ cm/s was achieved. Considering the TMP-001-loaded nanoparticles, 8.78±1.1% of the API was recovered that equals a permeation rate of $1.050 \pm 0.1332 * 10^{-4}$ cm/s. ANOVA declared no significant difference between the pure API and the nanoparticles carrying TMP-001 concerning their permeation rate ($p=0.166$). The spray dried formulation exhibited a lower permeation after 3.5 h of $0.815 \pm 0.0700 * 10^{-4}$ cm/s. This value was found to be significantly reduced compared to the pure API ($p=0.013$) and may indicate a sustained release of the API. Pictures taken by CLSM declared an accumulation of the Eudragit® RS 100-nanoparticles on the mucosal site of the cell layer. Augmentation of the nanocarrier concentration from 10 to 20 µg/mL led to an increased amount of nanoparticles represented in the cytoplasm of the cells composing the T-84-cell layer (see Fig. 3c and d).

Release Experiments Performed in the Biorelevant Medium FaSSIF V2

Further investigation on API-polymer interactions was accomplished by biorelevant release testing. Filter adsorption of the API was found to be negligible (lower than 1%). The extent and rate of release of an API from the formulation complements the perceptions gained with the Ussing chamber model. Dissolution profiles resulting from the sample-and-separate technique could not discriminate between the pure API TMP-001 and the nanosized formulation. A very fast release was determined suggesting a poor API-polymer interaction. The spray dried formulation exhibited a slower release profile (see Fig. 5).

DISCUSSION

Numerous authors have described polymeric nanoparticles as a promising tool for the controlled delivery of various compounds to their site of action (3,36,37) and have outlined the importance of physicochemical properties concerning their fate in the GI tract (16,36,37). Especially particle size, surface charge and the ability to interact with the mucosal surface define their transit time and potential to be taken up by specific cell types (8,16,37). However, very often the interaction of API and polymer as a crucial factor for drug release is neglected, although it is evident that a fast release of the API will lower the beneficial effect the polymeric shell implies (38,39). Eudragit® RS 100 is a positively charged polymethacrylic acid containing quaternary ammonium group. The electrostatic interactions between the polymer and functional groups of the API (e.g. carboxyl or hydroxyl groups) can influence the release behavior profoundly (39,40). After all, more often the polymer is used in matrix formulations where release is controlled by the length of diffusion pathways as observed for microparticles or pellet formulations (41,42).

Especially in the treatment of inflammatory bowel disease, a local accumulation at the ulcerated or inflamed tissues is beneficial and has been addressed by a multitude of studies. Nanoparticles with a size of approximately 240 nm containing budensonide in an Eudragit® S-coated poly(lactic-co-glycolic) acid matrix exhibited an elevated-accumulation at the site of inflammation in the lower GI tract of mice with an experimentally induced colitis. The anti-inflammatory properties of the API were significantly improved compare to the unprocessed API due to an enhanced penetration into the inflamed tissue (27). With prednisolone another potent anti-inflammatory compound was formulated by conjugation to chitosan as described by Onishi (43). Microparticles were subsequently obtained by emulsification and evaporation and coated with Eudragit® L and exhibited an altered distribution in the GI tract compared to the unprocessed API. The distal small intestine and the cecum were consequently exposed to a higher amount of the API and the systemic availability in rats was attenuated (43). Similar strategies have been considered for the treatment of colon cancer. By nanoencapsulation of

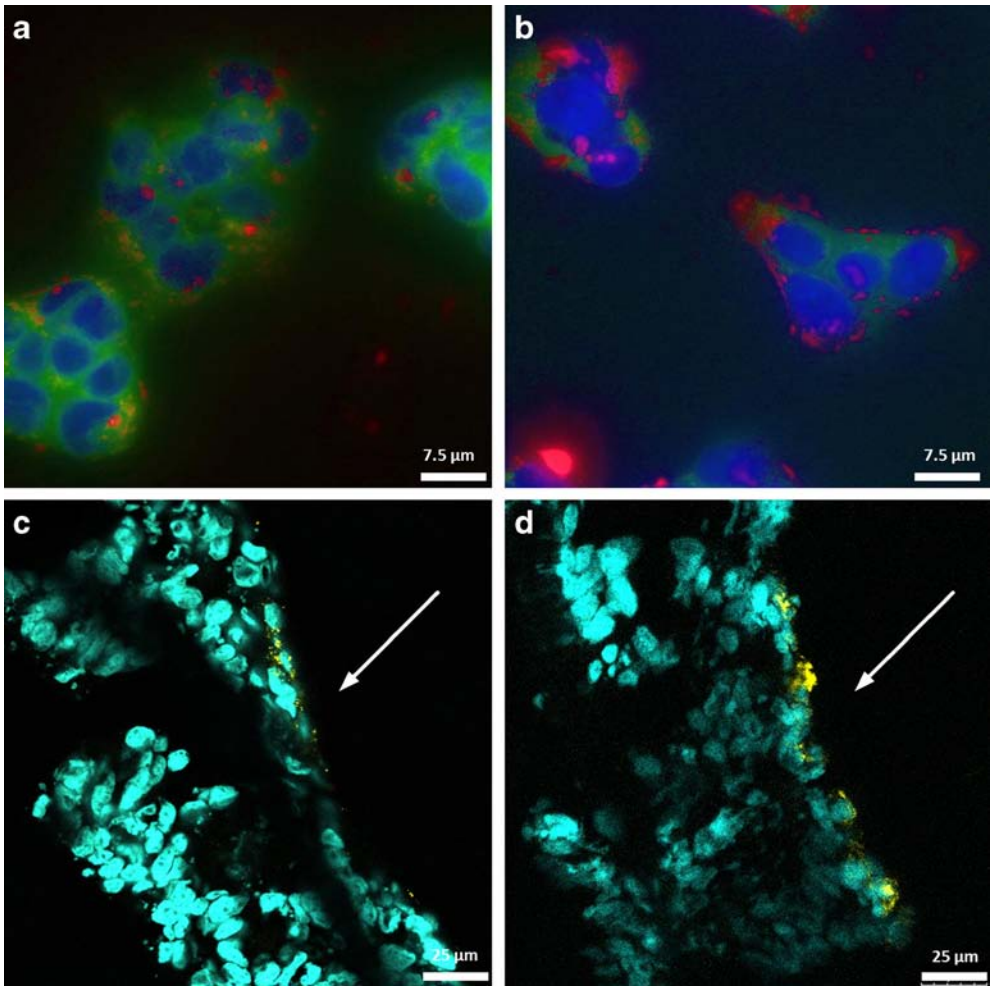

Fig. 3 (**a**) and (**b**) Fluorescence microscopy of Caco-2 cell layers that were incubated with unloaded Eudragit® RS 100 nanoparticles (**a**) or TMP-001-loaded Eudragit® RS 100 nanoparticles (**b**) at a concentration of 50 µg/mL. Nanoparticles appear red due to staining with the dye Lumogen® F Red 305, the cell membrane was *stained green* with Alexa® Fluor 488-Concanavalin A, the blue color represent the nucleus as a result of DAPI staining; (**c**) and (**d**) CLSM of cryoembedded T-84 cell layers obtained from the Ussing chamber experiments after incubation with nanocarrier suspensions. Unloaded Eudragit® RS 100 nanoparticles that were stained with Lumogen® F Orange 240 were applied at concentrations of 10 µg/mL (**c**), or 20 µg/mL (**d**), respectively. Nanoparticles can be recognized by their *orange/yellow* color. The clear fluorescence signal on the mucosal site indicates the accumulation of nanoparticles in this area that is correlated to a strong mucus interaction.

the photosensitizer temoporfin into Eudragit® RS 100 nanocarriers, the toxicity of the API was effectively reduced while the efficacy remained unaffected (20). A strong interaction of API and polymer resulted in sustained release properties of the final formulation design (20).

However, the recent investigations on Eudragit® RS 100-based formulations containing the anti-inflammatory compound TMP-001 focused on the interplay between drug release and the performance of nanocarriers as drug delivery devices in the GI tract. A broad spectrum of analytical methods was applied to this issue. The compound TMP-001 was effectively encapsulated into the carrier material by using the established nanoprecipitation technique. Recently, scale-up of this preparation method to medium-scale manufacture has been demonstrated (20).

TMP-001-loaded nanocarriers were characterized for their cytotoxicity in a concentration range between 0.05 and 3.00 mg of nanoparticles per mL medium. The selected concentrations corresponded to previous observations focusing on the safety of polymethacrylic-based formulations in monocytes and cancer cell lines (4,32,33). Even with the highest concentration no significant reduction of cell viability was observed.

Unfortunately, these findings were not accompanied by an improved efficacy of the API. A reduction of drug activity was excluded by assessing COX-2 inhibition for S-TMP-001-loaded nanoparticles which was comparable to the unprocessed API. Therefore, an initial burst release of the compound from the nanocarrier was assumed.

Poly(acrylic acids) have been described to apply for passive cell targeting resulting from interactions of positively-charged polymer with the cell membrane as a counterpart carrying negative charge (16,44). An intracellular accumulation of the drug delivery system was confirmed by a combination of fluorescence microscopy and flow cytometry. The internalization of Eudragit® RS 100-nanoparticles into the cytoplasm was visualized by TEM.

Moreover, CLSM pictures of the cryoembedded T-84 cell layers prepared for the Ussing chamber experiments, assured a pronounced accumulation of Eudragit® RS 100-nanoparticles on the mucosal site of the cell layer and their accumulation in the cytoplasm. Since those cells produce mucus, the local treatment of superficial inflammations or tumors in the GI tract is rendered possible by peroral administration of the presented nanocarrier design and remains unaffected

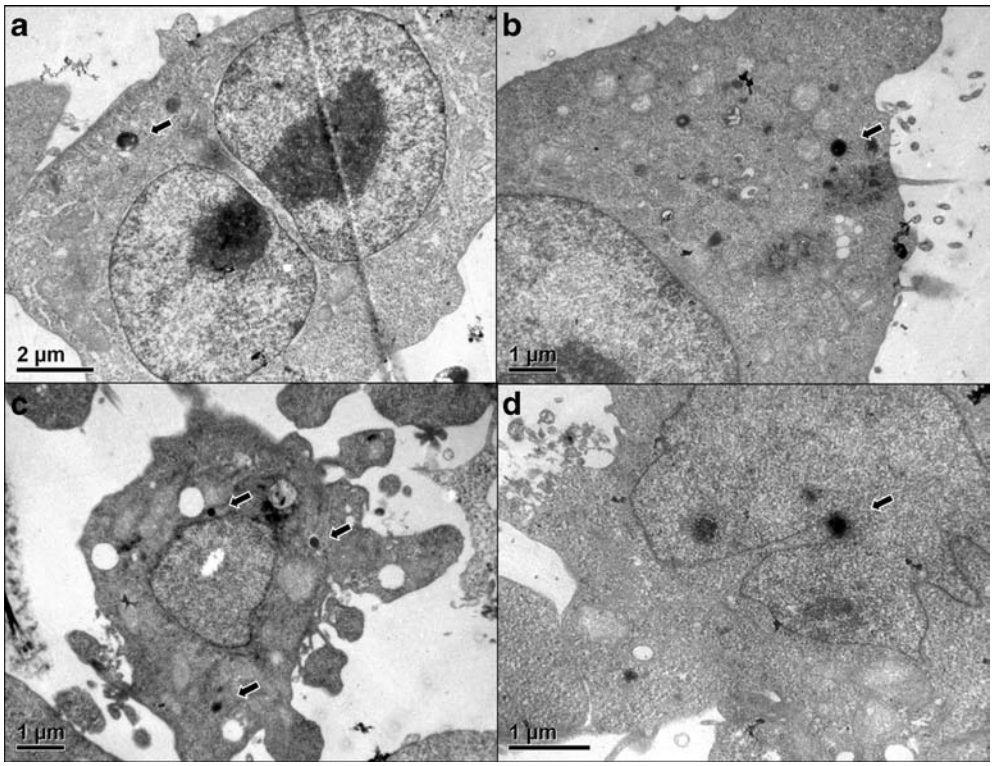

Fig. 4 Eudragit® RS 100-nanoparticles in the cytoplasm of Caco-2 cells. 50,000 cells were incubated with 50 μg nanoparticle supension for 2 h. After fixation, cutting with a microtome and a diatom knife, and a double staining procedure was performed. Nanoparticles in the cytoplasm were recognized and marked with the arrow symbol.

by interactions with the secreted glycoproteins. However, those findings also indicate that not the nanosphere itself is transported across the intestinal barrier, but the released API.

Therefore, both aspects, the release of the API from the nanocarrier matrix and the interaction of particles with biological surfaces define the therapeutic potential for a local treatment in the GI tract, which was pronounced for the TMP-001-loaded Eudragit® RS 100-nanoparticles.

Furthermore, the distinct uptake of nanocarriers into cells did not impact permeation of TMP-001 through the intestinal cell layer, suggesting an influence of release properties on the body distribution profile. A high permeability of the TMP-001-loaded formulation as indicated by a permeation rate of $1.050 \pm 0.1332 * 10^{-4}$ cm/s after 3.5 h was determined with the Ussing chamber model.

A T-84 cell line was used to simulate the most relevant characteristics of the human intestine, e.g., with regards to mucus secretion (45). Since Eudagit® RS 100-nanoparticles are well-known for their mucoadhesive behavior, the interaction of the positively charged nanosized formulation with a mucus-covered barrier, that is characterized by a negative charge, was studied (12).

The presence of mucus has been described as a triggering factor concerning the release properties of polymethacrylic-based formulations (5). Therefore, the evaluation of permeability was performed under conditions that simulate the most important morphological and functional aspects in the GI tract. T-84 cells are a robust model and can be applied to formulation and permeability screening without further processing or complex seeding procedures. A tight cell layer is formed, producing a thin layer of mucin (46) with a composition closely related to the one seen in the human intestine (47). In contrast to co-cultures, e.g., of Caco-2 and HT29 cells (48), which provide deeper insights into the mechanisms of colloid-surface interaction at the human gut wall, culturing techniques for T-84 cells are relatively simple assuring shorter preparation times and a standardized measurement.

Since the unprocessed API exhibited a comparable permeability combined with a high dissolution rate in FaSSIF V2, it

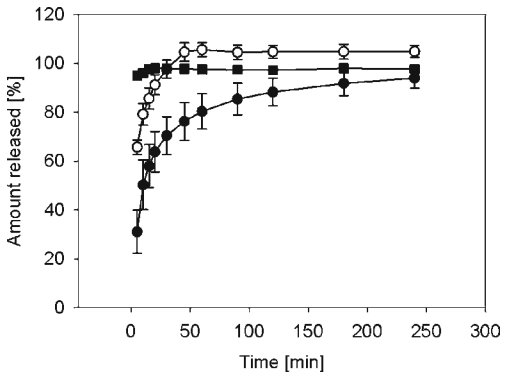

Fig. 5 Cumulative amount released in FaSSIF V2 of TMP-001 (*white circle*), TMP-001-loaded nanoparticles (*black square*), and the spray dried powder (*black circle*). An amount of 10 mg of API or the corresponding amounts of the formulations were tested. All experiments were performed in triplicate. S.D. is used for descriptive *error bars*.

is suggested that this was rather related to the physicochemical properties of the API (BCS class II). Hence, the poor interaction of API and polymer is prone to affect the *in vivo*-performance crucially.

Taking into account that there is no standard method established for release testing of API from nanoparticles, the sample-and-separate method with a low filter pore size (0.1 μm), appeared robust enough to exclude interference between the drug and the filter membrane (49). The filter adsorption of the API was tested prior to the release experiments.

Astonishingly, although Eudragit® RS 100 is a polymer with strong retardation features, no sustained release of TMP-001 could be observed. Therefore, it is concluded that the functional groups present in Eudragit® RS 100 (e.g., quaternary ammonium groups, esters, alkyl groups) show only weak interaction with TMP-001 compared to other drugs. Recently, a sustained drug release from Eudragit® RS 100 has been demonstrated for the photosensitizer temoporfin by our group (20). This API is characterized by a planar chlorin structure and hydroxyl groups. Assuming the degradation of the polymeric network to be comparable for both formulations, the binding force of API and polymer is considered to be much lower for TMP-001.

However, for both formulations a high drug loading efficiency has been achieved. Hence, adsorption of TMP-001 to the large surface area was assumed causing the instant release profile. Modification of diffusion pathways combined with an increase of particle size might be an approach towards controlling the release effectively. However, in this case the potential for passive drug targeting might be attenuated.

The nanosized formulation containing TMP-001 was processed further by spray drying. Adapting process parameters accurately, allowed the solidification of the aqueous nanosized suspension with a recovery rate of 94.2±5.9% referring to the API. Images taken by electron microscopy revealed a broader size distribution and an enlargement of particles but a preserved spherical shape. Moreover, there were still particles observed that exhibited the original diameter (<200 nm). Having transformed the particles by employing spray drying, the slope in the release profile in FaSSIF V2 was lowered. The permeability tested in the Ussing chamber model was still high, but significantly reduced compared to the pure API which further indicated sustained release properties. Taking into account those results, a diffusion-controlled release mechanism can be suggested. With increasing particle size a retardation of drug release was observed.

CONCLUSION

The presented research profoundly evaluates the interplay of physicochemical properties of polymethacrylic-based nanosized formulations and their applicability for diseases requiring a local treatment in the GI tract. On this basis, biorelevant release testing has been applied to the development of a nanosized drug delivery system intended for the controlled release of an anti-inflammatory compound at the specific site of action.

The internalization of Eudragit® RS 100-nanoparticles into the cells was assured by flow cytometry, CLSM and TEM-technique and declared an effective accumulation of nanocarriers at the target site.

However, nanoencapsulation was not sufficient to control the release properties of TMP-001. The developed formulation exposed an instant release and a high permeability of the API in the Ussing chamber model ($1.050 \pm 0.1332 * 10^{-4}$ cm/s). By applying spray drying to the formulation design, the release could be controlled by prolonging diffusion pathways into the micrometer range. However, the increased particle size and broadened size distribution will impact the capability of the drug delivery system for passive targeting applications and penetration depth into the mucin layer (11,12). This suggests that TMP-001 undergoes a diffusion-controlled release mechanism from the respective polymer which was not sufficient to control the availability of the compound in the GI tract effectively when nanoparticles were used.

Still a mucosal accumulation of the nanocarrier system regarding the cellular barrier in the Ussing chamber model, provided evidence for Eudragit® RS 100-nanoparticles as a suitable formulation system for the local treatment in the GI tract due to a pronounced mucus interaction. Furthermore, the impact of release properties on drug targeting strategies has been confirmed by the present investigation.

ACKNOWLEDGMENTS AND DISCLOSURES

This work has been supported by the Else Kröner-Fresenius Foundation (EKFS), Research Training Group Translational Research Innovation—Pharma (TRIP). Moreover, the authors acknowledge LOEWE initiative of the State of Hessen for financial support to the Research Center for Translational Medicine and Pharmacology. The analytical part of this work was supported by the DFG (German Research Association) grant SFB1039 Z01. The authors want to acknowledge Prof. Jennifer B. Dressman and Prof. Dieter Steinhilber for their support.

REFERENCES

1. Gaumet M, Gurny R, Delie F. Interaction of biodegradable nanoparticles with intestinal cells: the effect of surface hydrophilicity. Int J Pharm. 2010;390(1):45–52.

2. Gratton SE, Ropp PA, Pohlhaus PD, Luft JC, Madden VJ, Napier ME, *et al.* The effect of particle design on cellular internalization pathways. Proc Natl Acad Sci U S A. 2008;105(33):11613–8.
3. Kreuter J. Peroral administration of nanoparticles. Adv Drug Deliv Rev. 1991;7(1):71–86.
4. Niebel W, Walkenbach K, Beduneau A, Pellequer Y, Lamprecht A. Nanoparticle-based clodronate delivery mitigates murine experimental colitis. J Control Release. 2012;160(3):659–65.
5. Pridgen EM, Alexis F, Farokhzad OC. Polymeric nanoparticle technologies for oral drug delivery. Clin Gastroenterol Hepatol. 2014;12(10):1605–10.
6. Lamprecht A, Schafer U, Lehr CM. Size-dependent bioadhesion of micro- and nanoparticulate carriers to the inflamed colonic mucosa. Pharm Res. 2001;18(6):788–93.
7. Rabiskova M, Bautzova T, Gajdziok J, Dvorackova K, Lamprecht A, Pellequer Y, *et al.* Coated chitosan pellets containing rutin intended for the treatment of inflammatory bowel disease: in vitro characteristics and in vivo evaluation. Int J Pharm. 2012;422(1-2):151–9.
8. Lai SK, Wang Y-Y, Hanes J. Mucus-penetrating nanoparticles for drug and gene delivery to mucosal tissues. Adv Drug Deliv Rev. 2009;61(2):158–71.
9. Plapied L, Vandermeulen G, Vroman B, Preat V, des Rieux A. Bioadhesive nanoparticles of fungal chitosan for oral DNA delivery. Int J Pharm. 2010;398(1–2):210–8.
10. Tang BC, Dawson M, Lai SK, Wang YY, Suk JS, Yang M, *et al.* Biodegradable polymer nanoparticles that rapidly penetrate the human mucus barrier. Proc Natl Acad Sci U S A. 2009;106(46):19268–73.
11. Ensign LM, Cone R, Hanes J. Oral drug delivery with polymeric nanoparticles: the gastrointestinal mucus barriers. Adv Drug Deliv Rev. 2012;64(6):557–70.
12. Cone RA. Barrier properties of mucus. Adv Drug Deliv Rev. 2009;61(2):75–85.
13. Lautenschläger C, Schmidt C, Fischer D, Stallmach A. Drug delivery strategies in the therapy of inflammatory bowel disease. Adv Drug Deliv Rev. 2014;71:58–76.
14. Rajapaksa TE, Stover-Hamer M, Fernandez X, Eckelhoefer HA, Lo DD. Claudin 4-targeted protein incorporated into PLGA nanoparticles can mediate M cell targeted delivery. J Control Release. 2010;142(2):196–205.
15. Schmidt C, Lautenschlaeger C, Collnot EM, Schumann M, Bojarski C, Schulzke JD, *et al.* Nano- and microscaled particles for drug targeting to inflamed intestinal mucosa: a first in vivo study in human patients. J Control Release. 2013;165(2):139–45.
16. Desai MP, Labhasetwar V, Walter E, Levy RJ, Amidon GL. The mechanism of uptake of biodegradable microparticles in Caco-2 cells is size dependent. Pharm Res. 1997;14(11):1568–73.
17. Lehr C-M, Bouwstra JA, Tukker JJ, Junginger HE. Intestinal transit of bioadhesive microspheres in an in situ loop in the rat—a comparative study with copolymers and blends based on poly(acrylic acid). J Control Release. 1990;13(1):51–62.
18. Wacker M. Nanocarriers for intravenous injection-the long hard road to the market. Int J Pharm. 2013;457(1):50–62.
19. Agüeros M, Ruiz-Gatón L, Vauthier C, Bouchemal K, Espuelas S, Ponchel G, *et al.* Combined hydroxypropyl-β-cyclodextrin and poly(anhydride) nanoparticles improve the oral permeability of paclitaxel. Eur J Pharm Sci. 2009;38(4):405–13.
20. Beyer S, Xie L, Grafe S, Vogel V, Dietrich K, Wiehe A, *et al.* Bridging laboratory and large scale production: preparation and in vitro-evaluation of photosensitizer-loaded nanocarrier devices for targeted drug delivery. Pharm Res. 2015;32:1714–26.
21. Dressman JB, Berardi RR, Elta GH, Gray TM, Montgomery PA, Lau HS, *et al.* Absorption of flurbiprofen in the fed and fasted states. Pharm Res. 1992;9(7):901–7.
22. Moulari B, Beduneau A, Pellequer Y, Lamprecht A. Lectin-decorated nanoparticles enhance binding to the inflamed tissue in experimental colitis. J Control Release. 2014;188:9–17.
23. Lee SH. Intestinal permeability regulation by tight junction: implication on inflammatory bowel diseases. Intest Res. 2015;13(1):11–8.
24. Oleinick NL, Evans HH. The photobiology of photodynamic therapy: cellular targets and mechanisms. Radiat Res. 1998;150(5 Suppl):146–56.
25. Crcarevska MS, Dodov MG, Goracinova K. Chitosan coated Ca–alginate microparticles loaded with budesonide for delivery to the inflamed colonic mucosa. Eur J Pharm Biopharm. 2008;68(3):565–78.
26. Soppimath KS, Aminabhavi TM, Kulkarni AR, Rudzinski WE. Biodegradable polymeric nanoparticles as drug delivery devices. J Control Release. 2001;70(1–2):1–20.
27. Ali H, Weigmann B, Neurath MF, Collnot EM, Windbergs M, Lehr CM. Budesonide loaded nanoparticles with pH-sensitive coating for improved mucosal targeting in mouse models of inflammatory bowel diseases. J Control Release. 2014;183:167–77.
28. des Rieux A, Ragnarsson EG, Gullberg E, Preat V, Schneider YJ, Artursson P. Transport of nanoparticles across an in vitro model of the human intestinal follicle associated epithelium. Eur J Pharm Sci. 2005;25(4–5):455–65.
29. Dressman JB, Reppas C. In vitro-in vivo correlations for lipophilic, poorly water-soluble drugs. Eur J Pharm Sci. 2000;11(2):S73–80.
30. Lobenberg R, Amidon GL. Modern bioavailability, bioequivalence and biopharmaceutics classification system. New scientific approaches to international regulatory standards. Eur J Pharm Biopharm. 2000;50(1):3–12.
31. Akhlaq M, Khan GM, Wahab A, Khan A, Hussain A, Nawaz A, *et al.* A simple high-performance liquid chromatographic practical approach for determination of flurbiprofen. J Adv Pharm Technol Res. 2011;2(3):151–5.
32. Ronzani C, Safar R, Diab R, Chevrier J, Paoli J, Abdel-Wahhab MA, *et al.* Viability and gene expression responses to polymeric nanoparticles in human and rat cells. Cell Biol Toxicol. 2014;30(3):137–46.
33. Safar R, Ronzani C, Diab R, Chevrier J, Bensoussan D, Grandemange S, *et al.* Human monocyte response to S-nitrosoglutathione-loaded nanoparticles: uptake, viability, and transcriptome. Mol Pharm. 2015;12(2):554–61.
34. Zensi A, Begley D, Pontikis C, Legros C, Mihoreanu L, Wagner S, *et al.* Albumin nanoparticles targeted with Apo E enter the CNS by transcytosis and are delivered to neurones. J Control Release. 2009;137(1):78–86.
35. Porsch B, Hillang I, Karlsson A, Sundelof LO. Ion-exclusion controlled size-exclusion chromatography of methacrylic acid-methyl methacrylate copolymers. J Chromatogr A. 2000;872(1–2):91–9.
36. des Rieux A, Fievez V, Garinot M, Schneider Y-J, Préat V. Nanoparticles as potential oral delivery systems of proteins and vaccines: a mechanistic approach. J Control Release. 2006;116(1):1–27.
37. Jung T, Kamm W, Breitenbach A, Kaiserling E, Xiao JX, Kissel T. Biodegradable nanoparticles for oral delivery of peptides: is there a role for polymers to affect mucosal uptake? Eur J Pharm Biopharm. 2000;50(1):147–60.
38. Castelli F, Messina C, Sarpietro MG, Pignatello R, Puglisi G. Flurbiprofen release from Eudragit RS and RL aqueous nanosuspensions: a kinetic study by DSC and dialysis experiments. AAPS PharmSciTech. 2002;3(2).
39. Narisawa S, Nagata M, Hirakawa Y, Kobayashi M, Yoshino H. An organic acid-induced sigmoidal release system for oral controlled-release preparations. 2. Permeability enhancement of Eudragit RS coating led by the physicochemical interactions with organic acid. J Pharm Sci. 1996;85(2):184–8.

40. Donbrow M, Hoffman A, Benita S. Gradation of microcapsule wall porosity by deposition of polymer mixtures (Eudragit RL and Eudragit RS). Phase separation of polymer mixtures and effects of external media and conditions on release. J Microencapsul. 1995;12(3):273–85.
41. Faisant N, Siepmann J, Benoit JP. PLGA-based microparticles: elucidation of mechanisms and a new, simple mathematical model quantifying drug release. Eur J Pharm Sci. 2002;15(4):355–66.
42. Mauludin R, Muller RH, Keck CM. Development of an oral rutin nanocrystal formulation. Int J Pharm. 2009;370(1–2):202–9.
43. Onishi H. Pharmacokinetic evaluation of chitosan-succinyl-prednisolone conjugate microparticles as a colonic delivery system: comparison with enteric-coated conjugate microparticles. Health. 2014;6(11):1286–95.
44. van der Lubben IM, Verhoef JC, Borchard G, Junginger HE. Chitosan for mucosal vaccination. Adv Drug Deliv Rev. 2001;52(2):139–44.
45. Navabi N, McGuckin MA, Linden SK. Gastrointestinal cell lines form polarized epithelia with an adherent mucus layer when cultured in semi-wet interfaces with mechanical stimulation. PLoS One. 2013;8(7).
46. Navabi N, McGuckin MA, Lindén SK. Gastrointestinal cell lines form polarized epithelia with an adherent mucus layer when cultured in semi-wet interfaces with mechanical stimulation. PLoS ONE. 2013;8(7), e68761.
47. McCool DJ, Marcon MA, Forstner JF, Forstner GG. The T84 human colonic adenocarcinoma cell line produces mucin in culture and releases it in response to various secretagogues. Biochem J. 1990;267(2):491–500.
48. Beduneau A, Tempesta C, Fimbel S, Pellequer Y, Jannin V, Demarne F, *et al*. A tunable Caco-2/HT29-MTX co-culture model mimicking variable permeabilities of the human intestine obtained by an original seeding procedure. Eur J Pharm Biopharm. 2014;87(2):290–8.
49. Junemann D, Dressman J. Analytical methods for dissolution testing of nanosized drugs. J Pharm Pharmacol. 2012;64(7):931–43.